Materials Research Bulletin 45 (2010) 1361–1367

Contents lists available at ScienceDirect

Materials Research Bulletin

journal homepage: www.elsevier.com/locate/matresbu

Reduction and adsorption of Pb^{2+} in aqueous solution by nano-zero-valent iron—A SEM, TEM and XPS study

Yunfei Xi [a,b,*], Megharaj Mallavarapu [a,b], Ravendra Naidu [a,b]

[a] Centre for Environmental Risk Assessment and Remediation (CERAR), University of South Australia, Mawson Lakes, SA 5095, Australia
[b] Cooperative Research Centre for Contamination Assessment and Remediation of the Environment (CRC CARE), University of South Australia, Mawson Lakes, SA 5095, Australia

ARTICLE INFO

Article history:
Received 23 October 2009
Received in revised form 17 June 2010
Accepted 18 June 2010
Available online 25 June 2010

Keywords:
Metals
Chemical synthesis
Electron microscopy
Photoelectron spectroscopy
X-ray diffraction
Microstructure
Surface properties

ABSTRACT

This study reports the synthesis, characterisation and application of nano-zero-valent iron (nZVI). The nZVI was produced by a reduction method and compared with commercial available ZVI powder for Pb^{2+} removal from aqueous phase. Comparing with commercial ZVI, the laboratory made nZVI powder has a much higher specific surface area. XRD patterns have revealed zero-valent iron phases in two ZVI materials. Different morphologies have been observed using SEM and TEM techniques. EDX spectrums revealed even distribution of Pb on surface after reaction. The XPS analysis has confirmed that immobilized lead was present in its zero-valent and bivalent forms. 'Core–shell' structure of prepared ZVI was revealed based on combination of XRD and XPS characterisations. In addition, comparing with Fluka ZVI, this lab made nZVI has much higher reactivity towards Pb^{2+} and within just 15 min 99.9% removal can be reached. This synthesized nano-ZVI material has shown great potential for heavy metal immobilization from wastewater.

1. Introduction

The presence of heavy metal ions, which are the most toxic inorganic pollutants in the environment especially in water system, is becoming a major concern due to their acute toxicity. These ions are usually from natural weathering processes and industries. Some of these ions can be very toxic even at very low concentration and their toxicity may increase with their accumulation in water and soil. Among these heavy metal ions, Pb^{2+} is one of the major environmental pollutants. It can be introduced to the water system through corrosion of household plumbing, effluents from lead smelters, battery manufacturers, mining and many other industries. The problems associated with heavy metal pollution could be reduced or minimized by precipitation, ultra-filtration, electrode-deposition, reverse osmosis, etc., but these processes have disadvantages such as high cost, generation of secondary pollutants and poor removal efficiency. Adsorption has been found to be an effective and economic method with high potential for the removal, recovery and recycle of metals from wastewater [1], although desorption is an issue. In the last decade, zero-valent iron (ZVI) has been increasingly used in ground water remediation and hazardous waste treatment. Laboratory studies have demonstrated that ZVI can effectively transform chlorinated solvents, organochlorine pesticides, PCBs, organic dyes and heavy metals [2–9] into nontoxic forms. These zero-valent iron (ZVI) materials were proposed as a reactive material in permeable reactive barriers (PRBs) due to its great ability in reducing and stabilizing different types of pollutants [10–12]. It has many advantages, such as nontoxic – as iron is abundant in nature, lower price and high activity. And this material with particle size at nano-scale could exhibit superior activity because of their larger surface area and higher reactivity [2]. However, there is significant scope for research on nano-ZVI particularly its ability to remove toxic heavy metals from wastewater.

In this study, sodium borohydride reduction method was used for nano-ZVI preparation with a view to testing the synthesized material for the removal of Pb^{2+} from aqueous phase under laboratory conditions. The material was also compared with a commercially available ZVI powder. X-ray photoelectron spectroscopy (XPS) was used for surface element investigation to determine the distribution and valence states of heavy metals and iron on ZVI material surface. A series of characterisation methods—XRD, surface analysing and SEM with EDX were carried out to characterise the surface properties of the prepared materials.

* Corresponding author at: Centre for Environmental Risk Assessment and Remediation (CERAR), University of South Australia, Mawson Lakes Boulevard, Mawson Lakes, SA 5095, Australia. Tel.: +61 8 8302 6232; fax: +61 8 8302 3786.
E-mail address: yunfei.xi@unisa.edu.au (Y. Xi).

0025-5408/$ – see front matter © 2010 Elsevier Ltd. All rights reserved.
doi:10.1016/j.materresbull.2010.06.046

2. Experimental

2.1. Materials

In this study, iron (II) chloride tetrahydrate ($FeCl_2{\cdot}4H_2O$) 99%, sodium borohydride ($NaBH_4$) 98.5%, absolute ethanol and hydrogen chloride were obtained from Sigma–Aldrich and used without further purification. A reduced iron powder was obtained from Fluka with a purity of 99%. Lead solutions of different concentrations were made by dilution of 10 g L^{-1} stock solution prepared from analytical grade $Pb(NO_3)_2$ with deionized water (MilliQ system) and the initial pH was adjusted using nitric acid and sodium hydroxide.

2.2. Preparation of nZVI

In a typical procedure of nZVI preparation, 21.36 g of $FeCl_2{\cdot}4H_2O$ was dissolved in a mixture of absolute ethanol and deionized water (96 mL ethanol + 24 mL H_2O), this mixture was denoted as solution A while 12.2 g of $NaBH_4$ was dissolved in 400 mL of H_2O to form 1 M solution, denoted as solution B. Then solution B was added drop by drop to solution A in a fume hood, the resulting reaction can be expressed as $Fe^{2+} + 2BH_4^- + 6H_2O \rightarrow Fe^0 + 2B(OH)_3 + 7H_2\uparrow$, black particles of nZVI appeared and then the mixture was further stirred for 2 h. Prepared iron powder was separated from the solution by centrifugation at 3000 rpm and then the sediment was washed with 400 mL ethanol twice and dried in a 50 °C oven without air evacuation overnight. The prepared sample was kept in vacuum desiccator prior to use. As reported in some literatures, using ethanol to wash samples instead of using water is critical in stabilizing ZVI against immediate oxidation [2,13], and drying in atmosphere oven has passivation effect for ZVI application which may otherwise catch fire on exposure to atmospheric oxygen [13].

2.3. Characterisation methods

The samples were pressed in stainless steel sample holders. X-ray diffraction (XRD) patterns were recorded using CuKα radiation (n = 1.5418 Å) on a Panalytical X'Pert diffractometer operating at 40 kV and 40 mA between 5° and 90° (2θ) at a step size of 0.0167°. Adsorption and desorption experiments using N_2 were carried out at 77 K on a Gemini 2380 surface analyser. Prior to each measurement the samples were degassed at 353 K for 24 h. The specific surface area (SA) was determined using multipoint BET method [14]. A Philips XL30 scanning electron microscope (SEM) with integrated energy dispersive X-ray analyser (EDX) system was used for morphological studies. Samples were dried at room temperature and sprinkled onto adhesive carbon tapes supported on metallic stub and then coated with carbon. A Philips CM 200 transmission electron microscope (TEM) at 200 KV was used to investigate the microstructure of the lab made nZVI. This nZVI material was dispersed in acetone and then dropped on carbon-coated films and dried at room temperature for TEM study. A PerkinElmer Optima 5300V optical emission spectrometer (ICP-OES) was employed to measure the residual metal ion concentrations. The pH of the solutions was measured with Thermo Orion pH meter with a glass electrode. The X-ray photoelectron spectroscopy (XPS) analyses were performed on a Kratos AXIS Ultra DLD with a monochromatic Al X-ray source at 130 W. Each analysis started with a survey scan from 0 to 1320 eV with a dwell time of 55 ms, pass energy of 160 eV at steps of 0.5 eV with three sweeps. For the high-resolution analysis, the number of sweeps was increased, the pass energy was lowered to 20 eV at steps of 100 meV, and the dwell time was changed to 158 ms with 8 sweeps for Fe, 332 ms with 8 sweeps for O and 397 ms with 5 sweeps for Pb respectively. Band component analyses were undertaken using the Jandel 'Peakfit' software package. This software enabled the type of fitting function to be selected and allows specific parameters to be fixed or varied accordingly. Band fitting was done using a Lorenz–Gauss cross-product function with the minimum number of component bands used for the fitting process.

2.4. Pb^{2+} removal tests

Because of the reliability and simplicity of batch model, adsorption measurements were carried out by a batch technique at room temperature. ZVI was weighed into 50 mL centrifuge tube containing 40 mL of metal ion solution of known concentration and pH. The initial pH of all heavy metal solutions were adjusted to about 4 by addition of dilute HNO_3 solution, as there is no precipitation of Pb^{2+} at this pH value. The solutions were equilibrated on a rotary shaker at room temperature. The adsorbent was separated using 0.45 μm PTFE syringe filter. Pb^{2+} concentrations in the supernatant liquid were determined using an ICP-OES. All assays were carried out in 2% nitric acid background. The residual amount of metal ions was calculated by the difference between the amount initially added and that of remaining following equilibration. Solid-phase loading of metal, q_e (mg/g) was computed from the mass balance: $q_e = V(C_i - C_e)/M$ where C_i and C_e are total dissolved and equilibrium liquid phase metal concentration (mg/L), respectively, and M is the dose of adsorbent (g/L), V is the volume of metal solution. All working solutions were prepared from lead stock solution diluted with deionized water and all experiments were carried out in duplicate.

3. Results and discussion

3.1. Characterisation of the synthesized material

The XRD patterns are shown in Fig. 1. Laboratory synthesized nZVI and commercially available ZVI both show strong reflections at about 2.01 Å and 2.03 Å, respectively, which is a characteristic

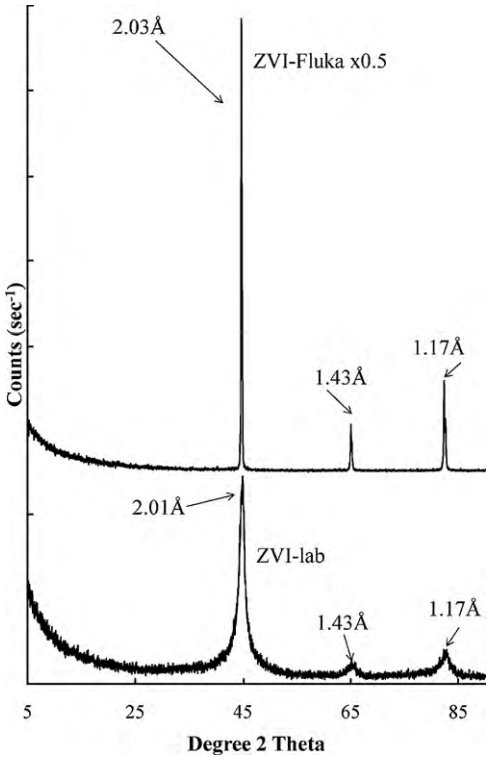

Fig. 1. XRD patterns of laboratory made nZVI and ZVI from Fluka.

reflection for ZVI [13] and is from the diffraction of 110 plane of Fe. This also indicates that for both ZVIs, Fe is mainly in its Fe0 state (only characterised by the basic reflection appearing at a 2-theta value of 44.8–44.7°) [15]. Some researchers have suggested a core–shell structure [7,15–18] where the Fe nanoparticles may form a core of main zero-valent iron with a shell made of iron oxides. Due to surface hydroxylation, FeOOH was also observed in some study [15], however, they were not detected in this study using XRD, which may due to the low crystallinity of iron oxides phases. Small reflections at about 1.43 Å (2 0 0 plane) and 1.17 Å (2 1 1 plane) were also observed on both samples from iron which was in accordance with the literature [19].

Adsorption and desorption experiments using N_2 were carried out at 77 K. The N_2 isotherms were used to calculate the specific surface area (SA) using multipoint BET [14] method. ZVI purchased from Fluka has a specific surface area only at 0.11 m^2/g, however, laboratory prepared nZVI showed a much higher specific surface area at 80.4 m^2/g.

The SEM images of Fluka ZVI and laboratory prepared nZVI are shown in Fig. 2a–c. The ZVI obtained from Fluka shows large particles with sizes at around several tens of microns with irregular shapes (Fig. 2a). Fig. 2b shows details of a Fluka ZVI particle at 10,000× magnifications which demonstrates solid and relatively smooth surface; this observation is also consistent with the small specific surface area (0.11 m^2/g) obtained from BET surface area analysis. The laboratory made iron particles as shown in Fig. 2c, however, demonstrates very different morphology where chain-like structure with floc aggregates can be observed similar to that reported by others [2,20]. The morphology and size difference of the two types of ZVIs also illustrate the large difference in surface areas obtained as discussed above.

3.2. Effect of Pb on the surface properties of the synthesized material

Fig. 2d shows the synthesized nZVI after reaction with Pb^{2+} and in this case, chain-like morphology is replaced with flakes/aggregates. This may be attributed to the formation of elemental lead and lead oxides via redox reaction, which changes the morphology of nZVI surface. Fig. 2e and f shows energy dispersive X-ray (EDX) spectrum of nZVI and nZVI reacted with Pb^{2+}. It was observed that peak from Pb was present after ZVI treatment with Pb from aqueous phase (in Fig. 2f, 2–3 KeV). Imaging of EDX (as shown in Fig. 3) further shows a series of elements distributions on the surface of material, where Fig. 3a shows a SEM image of the studied area, Fig. 3b shows the distribution of C element (shown by the bright points) which is mainly from the coating and adhesive carbon tape, as most of this element is observed not on the surface of nZVI. Fig. 3c and d shows the Fe K and Fe L signals, respectively,

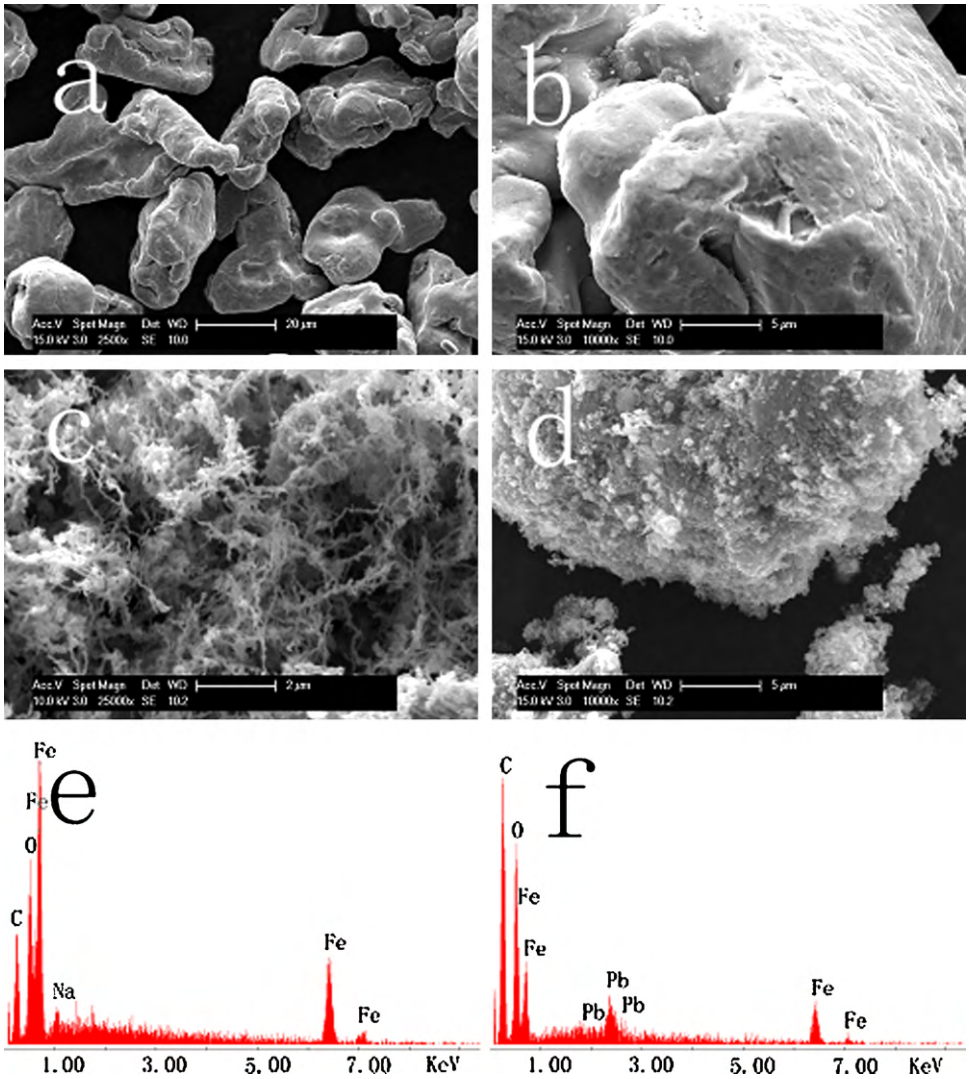

Fig. 2. (a) SEM image of Fluka ZVI; (b) Fluka ZVI–10,000× magnifications; (c) laboratory made nZVI; (d) laboratory made nZVI reacted with Pb^{2+}; (e) EDX element analysis of laboratory made nZVI; (f) EDX element analysis of laboratory made nZVI reacted with Pb^{2+}.

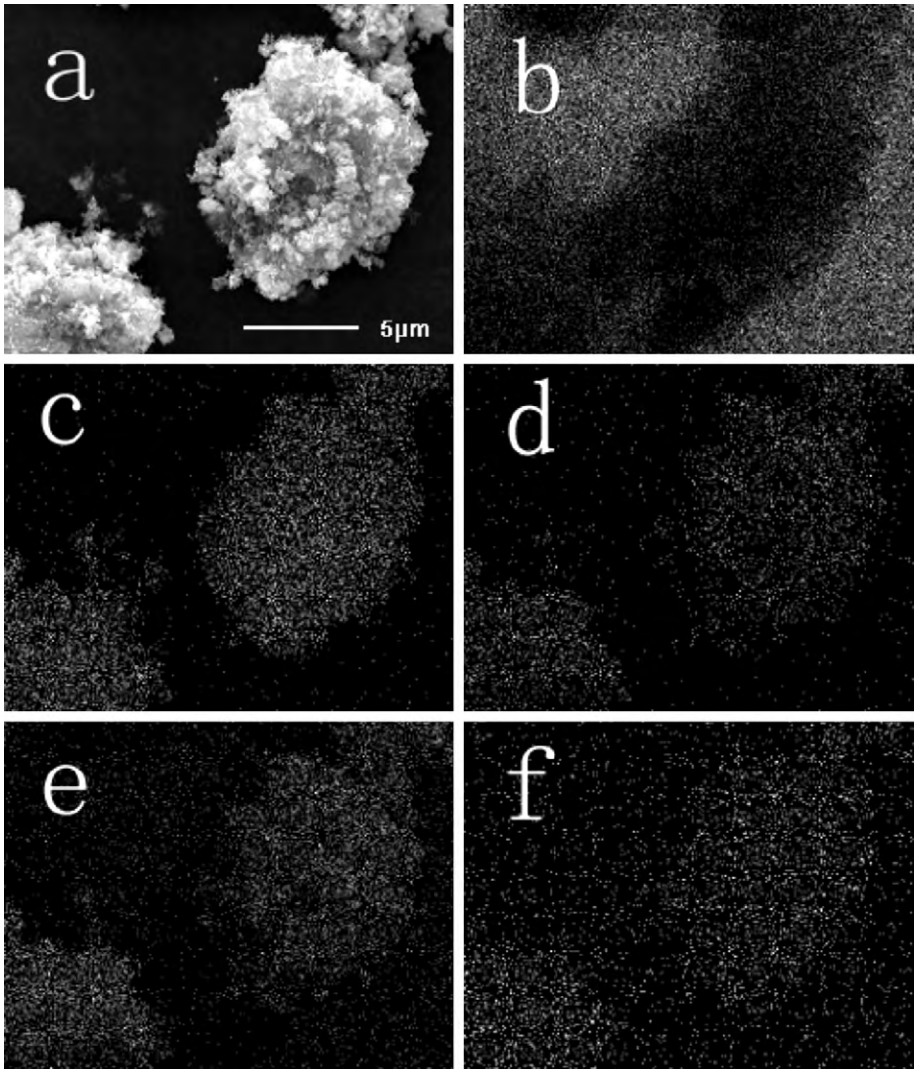

Fig. 3. (a) SEM image of a selected area of laboratory made nZVI reacted with Pb^{2+}; (b) EDX mapping of C (K) on this area; (c) EDX mapping of Fe (K) on this area; (d) EDX mapping of Fe (L) on this are; (e) EDX mapping of O (K) on this area; (f) EDX mapping of Pb (M) on this area.

Fig. 3e shows the signal of O K, and it also confirmed the existence of oxides. The oxides may come from iron oxides on nZVI surface and lead oxides after redox reaction. Even distribution of element Pb was observed on the surface of nZVI material as shown in Fig. 3f from Pb M signal. For comparison reason, Fig. 4a shows SEM image of a studied area of nZVI and its elements distributions (from Fig. 4b–f), respectively, where it can be observed that comparing with that of nZVI reacted with Pb^{2+}, distributions of elements of C, Fe, O are quite similar, except no Pb element distribution was observed on pure nZVI sample.

Fig. 5 shows the TEM image of the synthesized nZVI which permits the direct observation of microstructural features of this material confirming SEM observation of the presence of chain-like morphology from iron aggregations. It is likely that this type of chain is connected with pieces of iron and/or iron oxides particles, and the chain can be as long as several tens of microns (figure not shown).

3.3. Lead adsorption mechanism

It was reported in some literatures that nZVI can remove metal ions from aqueous solutions by various mechanisms including electrostatic adsorption, complex formation, reduction and precipitation [18,21]. In this study, redox reaction was expected to take place to a certain extent, as the standard reduction potential of Pb^{2+} (−0.13 V) is greater than that of Fe^{2+} (−0.44 V), insoluble Pb(0) may be observed on the surface of nZVI. XPS technique was applied to study the binding energy of element, which may be used as a 'fingerprint' for discrimination of different chemical environments of certain element. The XPS analysis in this study has firstly confirmed that lead on the surface of ZVI was present in both its zero-valent and bivalent forms. As shown in Fig. 6, the observed Pb 4f peaks are located at 136.2 and 137.2 eV, respectively, where the former value corresponds to the zero-valent Pb and the latter is from PbO, and these values are little lower than those obtained in a study [22], where 136.7, 138.1 eV were reported, respectively. While in Fig. 7, for nZVI reacted with Pb^{2+}, the photoelectron peak of O 1s can be decomposed into three peaks at 527.5, 528.7 and 530.3 eV, respectively which is in accordance with that in a literature, where these peaks represented binding energies of O^{2-}, OH^- and chemically or physically adsorbed water, respectively [23]. While for nZVI only, as shown in Fig. 8 the decomposed peaks from O 1s are located at 527.2, 528.6 and 530.0 eV, respectively. It can be observed that there was no significant shift of peak positions before and after ZVI reacted with Pb^{2+}. However, further examination of the peak area % using Peakfit software in this region suggested that there was noticeable change on area % of each decomposed peak. Area % can be used as a guide to calculate

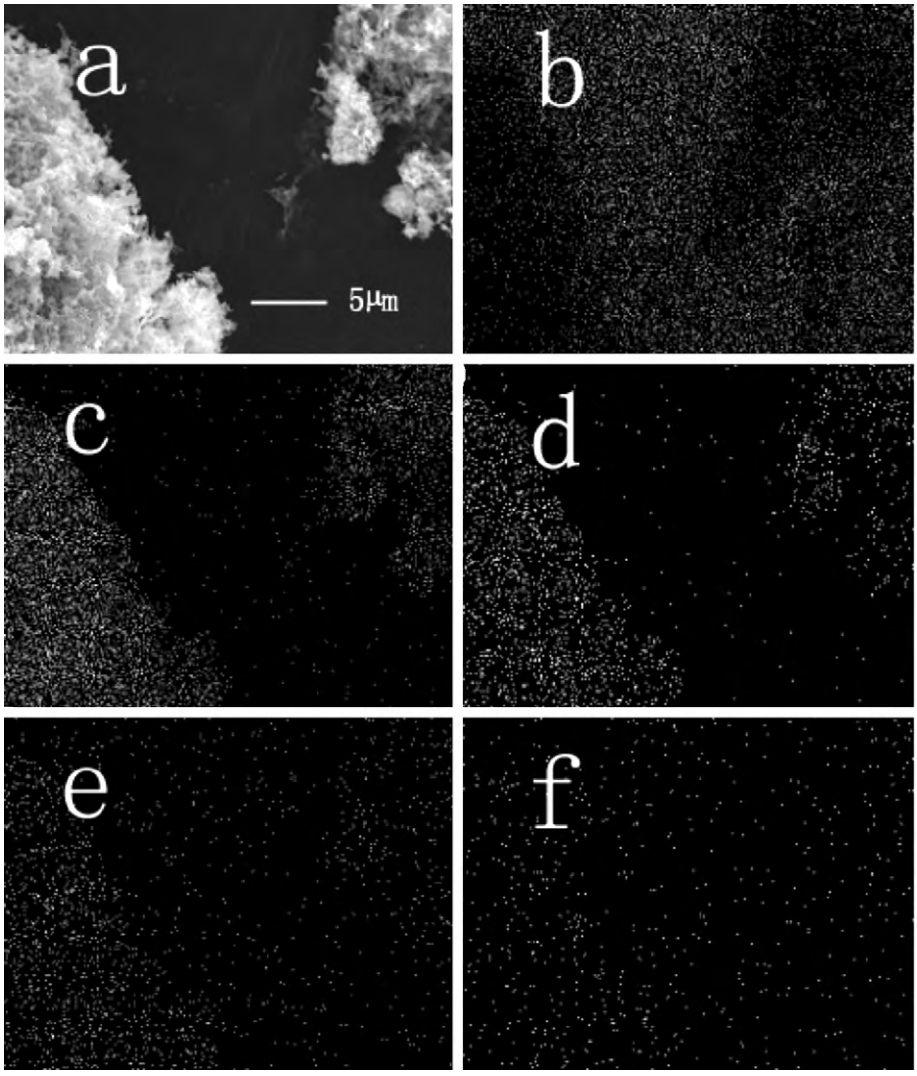

Fig. 4. (a) SEM image of a selected area of laboratory made nZVI; (b) EDX mapping of C (K) on this area; (c) EDX mapping of Fe (K) on this area; (d) EDX mapping of Fe (L) on this area; (e) EDX mapping of O (K) on this area; (f) EDX mapping of Na (K) on this area.

composition % change, because the number of photoelectron of a certain element is dependent on the atomic concentration of that element in the sample, so XPS can be used to quantify the relative chemical composition using the peak area. In this study, area % of O^{2-}, OH^- and H_2O of nZVI changed from 5.9%, 58.5% and 35.6%, respectively to 21.1%, 45.9% and 33%, respectively after its reaction with Pb^{2+}. It can be noticed that there was no significant change of area % on O 1s peak of water which only changed from 35.6% to 33% after reaction with Pb^{2+}. But area % of O 1s peak from O^{2-} increased from only 5.9% to 21.1%, which may be ascribed to the increased oxides percentage after nZVI reacted with Pb^{2+}, as lead oxide formed after reaction, so the percentage of this part increased

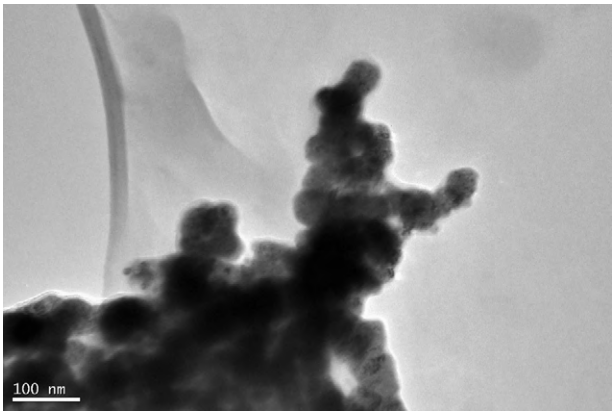

Fig. 5. TEM image of laboratory made nZVI.

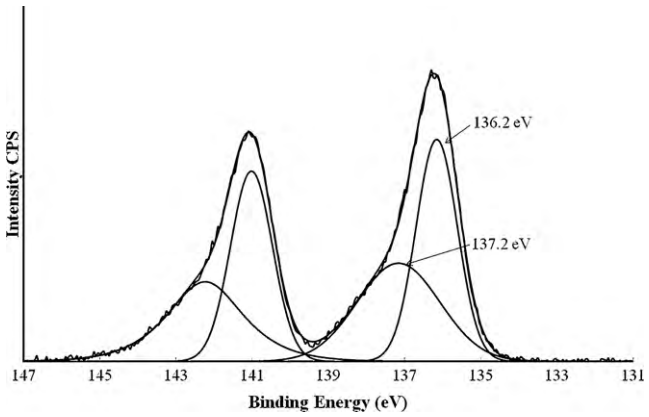

Fig. 6. XPS spectroscopy of Pb 4f in lab made nZVI reacted with Pb^{2+}.

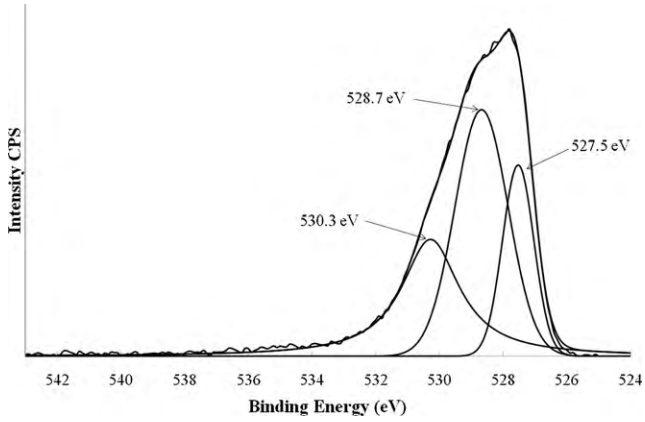

Fig. 7. XPS spectroscopy of O 1s in lab made nZVI reacted with Pb^{2+}.

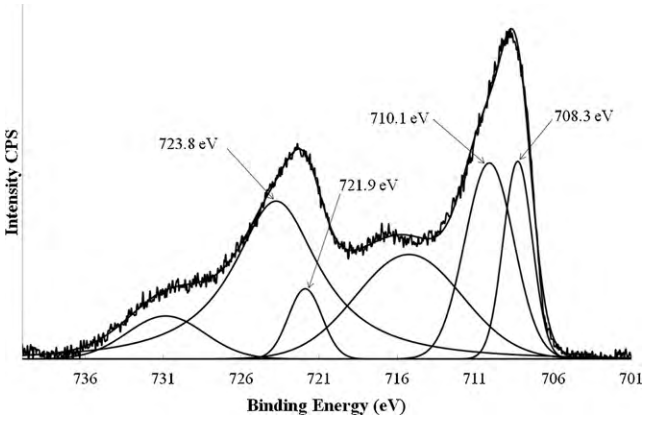

Fig. 9. XPS spectroscopy of Fe 2p in lab made nZVI.

significantly. Area % of peak at around 528 eV did not change a lot before and after reaction, which meant the FeOOH content % was relative stable. FeOOH was a result of surface hydroxylation and subsequent dehydration of the exposed shell when iron nanoparticles were in contact with aqueous solution [2]. Based on the discussion above, it could be suggested that Pb^{2+} undergo partial reduction following its immobilization on nZVI surface resulting in precipitation on the surface as PbO. The Fe 2p spectra consists of both 2p3/2 peaks at about 708 eV in binding energy (BE) and 2p1/2 at about 720 eV in BE, but both energies are lower than those reported in literature [18], where 711 and 725 eV were observed, respectively. In this study, it was noticed that the BE of Fe 2p3/2 peaks increased with Pb^{2+} immobilized on Fe surface, from 708.3 and 710.1 eV on ZVI as shown in Fig. 9 to 708.5 and 710.4 eV (see Fig. 10), respectively (towards higher BE). Where peak at 708.3 eV is ascribed to Fe_2O_3 + FeO, and after reaction with Pb, the peak at 708.5 is ascribed to Fe_2O_3. The peak at 710 eV is from Fe^{2+} and changed to Fe^{3+} at 710.4 eV after Pb immobilization.

A similar tendency is reported on Fe 2P1/2, where peaks at 721.9 and 723.8 eV (see Fig. 9) shifted to 722 and 723.9 eV (as shown in Fig. 10), respectively. It was reported that the binding energy of Fe will shift to higher BE with the decease of Fe content [24]. In this study, the Pb was immobilized on Fe surface and at the same time some iron ions were released to the solution (though only very small amount of Fe released, see details below), so the percentage of Fe content was decreased. Zero-valent iron peak at about 706.4–707 eV was not distinguished in the XPS spectrum, which may because XPS is a truly surface analysis technique with only 2–5 nm probing depth, however, this observation when combined with XRD results has strongly supported our speculation on 'core–shell' structure: because XRD and XPS techniques have individually proved the existence of Fe(0) and iron oxides, respectively. The reason for why iron oxide phase was not observed using XRD was because of its low crystallinity, at the same time, the reason why Fe(0) was not detected using XPS was because of the limitation of XPS technique – only a surface technique, so iron as 'core' was not detected in XPS. However, the combination of these two techniques together has strongly supported the 'core–shell' theory.

3.4. Pb removal tests results

For optimising adsorption time, at around pH 4 (no precipitation for Pb^{2+} at this value), a set of experiments were conducted by equilibrating 40 mL of 200 mg/L Pb^{2+} solution with 0.1 g of ZVI materials at 25 °C. Following equilibration for periods ranging from 15 min to 360 min, solution concentration of Pb^{2+} was determined to calculate immobilized Pb^{2+} on ZVIs. The effect of mixing time on removal density shows that only very small amount of Pb^{2+} (usually less than 2 mg/g) can be immobilized onto the commercial ZVI powder with increase in contact time (figure not shown). This demonstrated that commercial ZVI with large particles at micron level and very small surface area (only at 0.11 m^2/g) had very limited reactivity/adsorption capacity for Pb^{2+} at this pH value. However, the laboratory synthesized nZVI powder showed large capacity for Pb^{2+} immobilization with the amount of Pb removed being 99.9% within 15 min (figure not shown).

In order to optimise the amount of adsorbent/catalyst material required for most efficient removal of Pb^{2+} from aqueous solution, a series of experiments were undertaken with varying solid concentrations in the reaction mixtures containing 40 mL of 500 mg/L Pb^{2+} solution at pH 4. The Pb^{2+} concentrations were

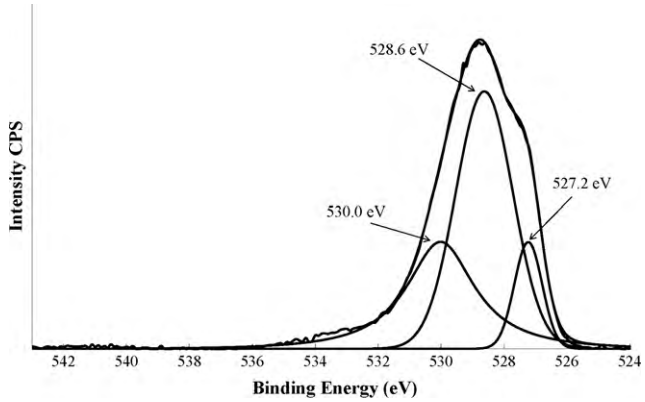

Fig. 8. XPS spectroscopy of O 1s in lab made nZVI.

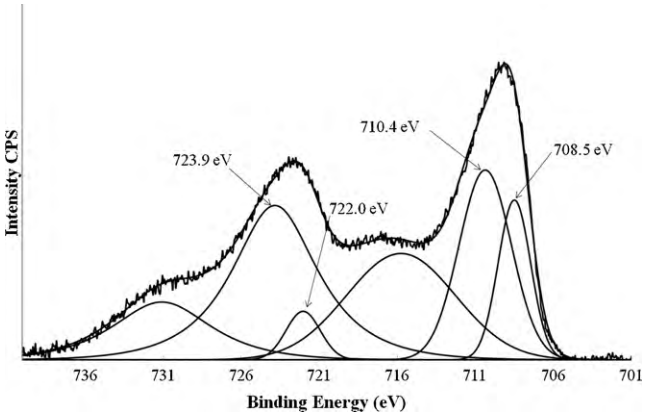

Fig. 10. XPS spectroscopy of Fe 2p in lab made nZVI reacted with Pb^{2+}.

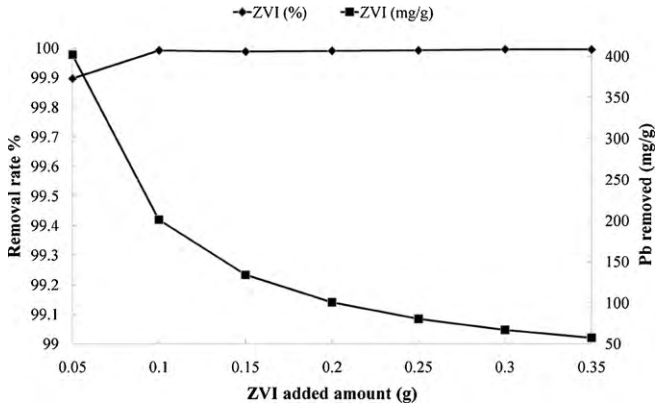

Fig. 11. Influence of added amount of nZVI on Pb^{2+} removal amount and % rate.

tested after 24 h of equilibration at 25 °C. The amount of Pb^{2+} adsorbed on the centrifuge tubes was found to be negligible. Relationship between the added laboratory made nZVI and the amounts of Pb^{2+} immobilized rates (%) are shown in Fig. 11. It was demonstrated that Pb^{2+} immobilized amount (mg/g) decreased with increasing adsorbent concentration (g). The rate of Pb immobilized (%) increased with an increase in the amount of adsorbent (g). As shown in Fig. 11, removal rate of Pb^{2+} on only 0.05 g of nZVI can reach up to >99%, which corresponds to 401.8 mg/g. And at the same time, though at acidic condition, the released iron concentration in solution after reaction is only from 0.27 mg/L (when 0.05 g of nZVI was added) to 0.75 mg/L (when 0.35 g of nZVI was added), which should not have any negative effects considering Fe is an abundant element in natural environment.

4. Conclusions

In this study, nano-zero-valent iron (nZVI) prepared using reduction method together with a commercially available ZVI (Fluka) was used for Pb^{2+} removal from aqueous phase.

- Compared to commercial ZVI (0.11 m^2/g), the laboratory made nZVI powder has much higher specific surface area, which is at 80.4 m^2/g as determined by BET method.
- XRD patterns have revealed iron phases in these two ZVI materials.
- SEM images have shown different morphologies between two ZVIs, where Fluka ZVI shows big particles with sizes at around several tens of microns with irregular shapes, the laboratory made iron particles, however, demonstrate chain-like structure with floc aggregates. And morphology of flakes/aggregates was observed after treated with Pb^{2+}.
- Energy dispersive X-ray (EDX) spectrum study shows even distribution of Pb on the surface.
- TEM image has confirmed the observation in SEM study.
- The XPS analysis confirmed that immobilized lead was present in its zero-valent and bivalent forms, and iron oxides were also detected. Based on both XRD and XPS results, 'core–shell' structure of ZVI was supported.
- Comparing with Fluka ZVI, this lab made nZVI had much higher reactivity towards Pb^{2+} at studied pH value and within just 15 min the removal rate at 99.9% can be reached. And material amount effect showed only 0.05 g of ZVI can remove Pb^{2+} at up to >99% (401.8 mg/g).

In summary, this study demonstrates a great potential for heavy metal immobilization using nano-zero-valent iron.

Acknowledgements

The authors would like to acknowledge the financial and infrastructural support of the Centre for Environmental Risk Assessment and Remediation (CERAR, University of South Australia) and the Cooperative Research Centre for Contamination Assessment and Remediation of the Environment (CRC CARE).

References

[1] S.E. Bailey, T.J. Olin, R.M. Bricka, D.D. Adrian, Water Res. 33 (1999) 2469–2479.
[2] C. Uzum, T. Shahwan, A.E. Eroglu, I. Lieberwirth, T.B. Scott, K.R. Hallam, Chem. Eng. J. 144 (2008) 213–220.
[3] K.J. Cantrell, D.I. Kaplan, T.W. Wietsma, J. Hazard. Mater. 42 (1995) 201–212.
[4] H.-H. Cho, J.-W. Park, Chemosphere 64 (2006) 1047–1052.
[5] T. Dombek, E. Dolan, J. Schultz, D. Klarup, Environ. Pollut. 111 (2001) 21–27.
[6] A. Ghauch, J. Rima, C. Amine, M. Martin-Bouyer, Chemosphere 39 (1999) 1309–1315.
[7] C. Noubactep, J. Hazard. Mater. 166 (2009) 79–87.
[8] C. Noubactep, A.M.F. Kurth, M. Sauter, J. Hazard. Mater. 169 (2009) 1005–1011.
[9] C. Noubactep, J. Hazard. Mater. 168 (2009) 1613–1616.
[10] M.M. Scherer, S. Richter, R.L. Valentine, P.J.J. Alvarez, Crit. Rev. Environ. Sci. Technol. 30 (2000) 363–411.
[11] A.B. Cundy, L. Hopkinson, R.L.D. Whitby, Sci. Total Environ. 400 (2008) 42–51.
[12] J.S. Ahn, C.-M. Chon, H.-S. Moon, K.-W. Kim, Water Res. 37 (2003) 2478–2488.
[13] O. Celebi, C. Uzum, T. Shahwan, H.N. Erten, J. Hazard. Mater. 148 (2007) 761–767.
[14] S. Brunauer, P.H. Emmett, E. Teller, J. Am. Chem. Soc. 60 (1938) 309–319.
[15] Y.-P. Sun, X.-Q. Li, J. Cao, W.-X. Zhang, H.P. Wang, Adv. Colloid Interface Sci. 120 (2006) 47–56.
[16] Y. Liu, H. Choi, D. Dionysiou, G.V. Lowry, Chem. Mater. 17 (2005) 5315–5322.
[17] J.T. Nurmi, P.G. Tratnyek, V. Sarathy, D.R. Baer, J.E. Amonette, K. Pecher, C. Wang, J.C. Linehan, D.W. Matson, R.L. Penn, M.D. Driessen, Environ. Sci. Technol. 39 (2005) 1221–1230.
[18] X.-Q. Li, W.-X. Zhang, J. Phys. Chem. C 111 (2007) 6939–6946.
[19] L.-H. Chen, C.-C. Huang, H.-L. Lien, Chemosphere 73 (2008) 692–697.
[20] Y.-P. Sun, X.-Q. Li, W.-X. Zhang, H.P. Wang, Colloids Surfaces A: Physicochem. Eng. Aspects 308 (2007) 60–66.
[21] C. Uzum, T. Shahwan, A.E. Eroglu, K.R. Hallam, T.B. Scott, I. Lieberwirth, Appl. Clay Sci. 43 (2009) 172–181.
[22] H. Abdel-Samad, P.R. Watson, Appl. Surf. Sci. 136 (1998) 46–54.
[23] X.-Q. Li, D.W. Elliott, W.-X. Zhang, Crit. Rev. Solid State Mater. Sci. 31 (2006) 111–122.
[24] A.N. Hattori, K. Hattori, H. Daimon, Surf. Interface Anal. 40 (2008) 988–992.